

Zahreddine Nafa · Mostefa Araar

Applied data for modeling the behavior in cyclic torsion of beams in glued-laminated wood: influence of amplitude

Received: May 21, 2001 / Accepted: January 9, 2002

Abstract We present some applied data concerning the torsional behavior of glued-laminated wood beams under several loading programs. These data can contribute to adequate modeling of such behavior. We review the theory of the structure and rheology of the wood material and the torsion of beams, particularly those that are anisotropic, and we describe the test device and the experimental environment that led to the data in question. We show the failure characteristics of the studied beams in monotonous torsion and the influence of the loading amplitude in cyclic torsion on their behavior.

Key words Wood · Cyclic loading · Glued-laminated · Beam · Torsion

Introduction

Although wood is the most ancient material used by humans for construction, it has remained the least known, essentially owing to the complexity of its structure and the weakness of its resistance features. The glued-laminated technique was developed at the beginning of the twentieth century with the aim of attenuating effects due to defects in the wood and to develop structural elements of significant size. Wood has been the object of various procedures applied separately or combined. The rational use of this material requires knowledge of its behavior. It is with this aim that our work was begun to investigate experimentally the behavior of glued-laminated beams in torsion.

Material wood

The macroscopic structure of wood is characterized by concentric annual rings of variable thickness due to the seasonal growth of the tree. Microscopic analysis has revealed that wood is composed of cellular elements, with different arrangements among species, associated with other elements such as resinous channels. The cell wall is essentially composed of cellulose, hemicelluloses, and lignin, polymers that play an important role in the rheological behavior of wood. The complexity of the wood structure, characterized by marked anisotropy and other constraints, induced industrialists to produce modified or reconstituted woods. The glued-laminated process constitutes the simplest way to attenuate effects due to defects in wood and to obtain important structural elements. A major constituent of the glued-laminated beam is the lamella. Lamellas, once dried, are planed and then, after gluing, are stacked. Jacks ensure tightening during the necessary time for the glue to hold. The complexity of the wood material requires a model for its examination that, without straying from the main features of its structure, facilitates such examination. The bark, containing natural growth defects such as knots, cracks, or eccentricities, is used by ignoring its singularities. On the other hand, a board cut far from the pith, which must logically refer to a cylindrical coordinate system in view of its geometry and its structural details such as cylindrical envelopes, is studied generally in a right-angled Cartesian system.^{1,2} Complementary to these hypotheses, one usually admits that wood is also a homogeneous, continuous body.³

Elastic behavior

Stress-strain curves resulting from mechanical testing of wood show a linear zone that varies depending on the test. The elastic model constitutes a powerful tool for wood. It can be applied with good success, in first approximation, for obtaining reasonable results. The anisotropic behavior of

Z. Nafa · M. Araar (✉)
Institute of Civil Engineering, University of Annaba, B.P.12, 23000
Annaba, Algeria
Tel. +213-3887-5397; Fax +213-3883-6617
e-mail: na_z@carmail.com

wood requires a more general formulation of Hook's law, as in Eqs. (1) and (2).

$$\sigma_{ij} = C_{ijkl} \cdot \varepsilon_{kl} \quad (1)$$

$$\varepsilon_{ij} = S_{ijkl} \cdot \sigma_{kl} \quad (2)$$

where σ_{ij} and ε_{ij} are components of stress and strain tensors, and C_{ijkl} and S_{ijkl} are components of rigidity and compliance tensors, respectively.

Much general work has been dedicated to characterizing the elastic behavior of wood,¹⁻³ and others have provided the elastic constants of the species or other studies based on classic or original measuring methods.³⁻⁹

Viscoelastic behavior

Studies on the elasticity of wood assume that the distortion is reversible, and that it remains constant over time if a constant load is maintained. However, when stress is applied, the first response is distortion of the elasticity that increases with time if the stress is maintained. This is called viscoelastic behavior. Such behavior appears in different ways: as creep under a constant load; as relaxation of stress under constant distortion; and as a damped dynamic response among others. To characterize the viscoelastic behavior of wood, some^{2,10-12} have proposed simple viscoelastic models that permit reconstitution of the wood's creep functions with a good approximation. Schniewind Barrett¹⁰ used a parabolic model of the type:

$$S(t) = S_0 + mt^n \quad (3)$$

proposed notably by Bodig and Jayne² and adopted by Cariou.¹² Foudjet¹³ used a model of the type

$$S(t) = a - be^{-t/t_1} - ce^{-t/t_2} \quad (4)$$

Other, more or less complicated models have been proposed to describe one, two, or three creep components.²

Cyclic behavior

The repetition of loading and unloading a specimen to a frequency lower than its own frequency is defined as *cyclic loading*. If the distortion of the body is elastic, features of material fatigue determine its resistance to the alternate loads; the failure occurs after a large cycle number. However, if the body sustains elastoplastic distortion, at a load lower than the limit one risks having a critical state for a number of cycles that is relatively little elevated. To the inverse of wood and for obvious grounds, materials used often as metallic alloys or those of high performance in the composites have been the object of advanced studies. The following observations have been made.

1. Three types of limit behavior are possible.
 - a. Adaptation, where the response becomes merely elastic
 - b. Accommodation, where the plastic distortion is periodic

- c. Ratchet, where the plastic distortion constantly progresses
2. The ratchet can result in instantaneous plastic phenomena as well as various viscous phenomena (e.g., creep)
 3. The limit state depends on loading speeds and temperatures.

Studies on wood cyclic behavior are rare; one can mention those done by King¹⁴⁻¹⁶ or Kellog.¹⁷ King studied repeated tension parallel to fibers in 11 wood species. He concluded that the maximum stress level for which residual distortions did not appear was roughly 42% (average) of the ultimate resistance, with individual values for each species varying between 21% and 80%. Kellog studied repeated tension on specimens from mine wood species; the experimental points have been smoothed by polynomial equations curves of the shape:

$$\Delta\varepsilon = a + N^b - c \quad (5)$$

where $\Delta\varepsilon$ is the creep; N the number of cycles; and a , b , and c are constants.

Torsion

Saint-Venant theory

The Saint-Venant theory consists in constructing a displacement field u that takes into account the transverse section rotations along the oz axis of the beam and their wrappings. It is defined by

$$\begin{aligned} \text{Displacements: } u &= -\theta zy \quad (6) \\ v &= +\theta zx \end{aligned} \quad (7)$$

which represents the rotation of the transverse section; θ is the rotated angle of the transverse section situated at a distance z from the origin.

$$\text{Displacement: } w = \theta \Psi(x,y) \quad (8)$$

which represents the transverse section warping definite by the function $\Psi(x,y)$. The state of stress and strain can be easily deduced from the supposed displacement field; and the resolution of the problem amounts to determining the warping function $\Psi(x,y)$ using equilibrium equations and boundaries conditions.

Rectangular section rod

Using the analogy of membrane distortion, Timoshenko and Goodier¹⁸ showed that the solution for a rectangular section is a convergent set shape.

They deduced the moment and the maximum stress expressions in the function of the section measurements:

$$\tau_{\max} = 2kG\theta a \quad M_t = k_1 G \theta (2a)^3 (2b) \quad (9)$$

$$\tau_{\max} = \frac{M_t}{k_2 (2a)^2 (2b)} \quad (10)$$

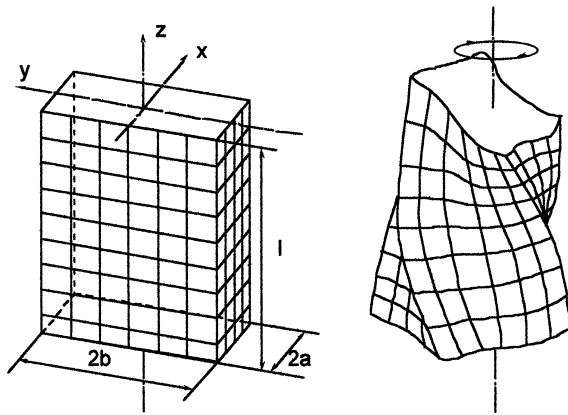


Fig. 1. Torsion of a prismatic rod

The numerical coefficients k , k_1 , and k_2 depend only on b/a (Fig. 1) and have been noted by authors such as Timoshenko and Goodier¹⁸ and Sokolnikoff.¹⁹

Experimental procedure

Specimens

The specimens used were small models of beams used for construction. They were 900mm long and were obtained by gluing together six lamellas of 40mm width and 10mm thickness. The wood used was spruce. Before preparing the specimens (beams), each lamella was measured for density and for Young and shear moduli. We composed the beams based on the shear modulus of the lamellas. As the number of lamellas to manage was high, a computer program was used for two reasons: (1) to have beams with a shear modulus with a fixed mean; and (2) to place the six lamellas in such a way that the beam was balanced from the point of view of rigidity. Once the beams were ready, we proceeded to the gluing. The adhesive used was Enocol RLF 185 of the Ceca Society (Paris). It is a mixture of resorcine, phenol, and formalin.

Machine and test installation

We developed and used an installation that permitted us to transform the straight movement of a jack to a rotary movement. The automation, surveillance of tests, and acquisition and saving of data were done on a computer.

Tests

A set of monotonous tests were done to measure the middle failure moments. Tests were conducted with controlled displacement with a gradient of $2^\circ/s$. Three test programs were used for the cyclic tests to determine the influence of the amplitude, the middle moment, and the maximum moment on the behavior of the beams. We report here only the first

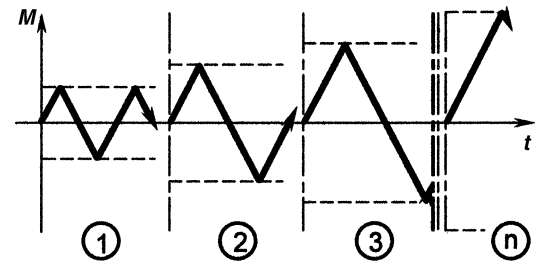


Fig. 2. Loading program

Table 1. Monotonous failure moment

Beam	Failure moment (Nm)	Average	Standard error
Batch 1			
S1.12	344.93	368.81	11.95
S1.17	381.34		
S1.4	380.16		
Batch 2			
S2.5	441.12	451.74	9.25
S2.19	443.95		
S2.27	470.16		
Batch 3A			
S3A.30	435.85	383.71	18.13
S3A.19	390.79		
S3A.34	404.72		
S3A.13	366.51		
S3A.17	343.34		
S3A.7	426.21		
S3A.23	419.68		
Batch 3B			
S3B.17	323.00	398.16	12.70
S3B.34	438.63		
S3B.24	404.59		
S3B.6	367.09		
S3B.3	349.50		
S3B.25	419.44		

program, which consisted of a set of tests where the middle moment was held at nil, and we varied the loading amplitude (Fig. 2). The other parameters will be reported in another paper.

Specimens of various available batches were distributed between monotonous and cyclic tests arbitrarily. Specimens are designated $S_{i,j}$, where i is the batch number and j is the specimen number.

Results and discussion

Monotonous tests

Results of the monotonous tests are in Table 1. During the test the beam first was distorted elastically. A crack then appeared in the middle of the beam's large face and propagated longitudinally until ultimate failure of the beam (Fig. 3). The $M-\theta$ curves are of the shape indicated in Fig. 4, where one can note the quasi-fragile character of the beam's behavior in monotonous torsion.

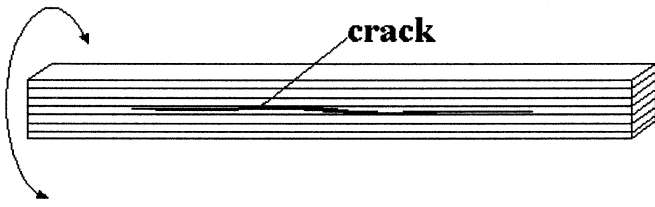


Fig. 3. Crack leading to failure

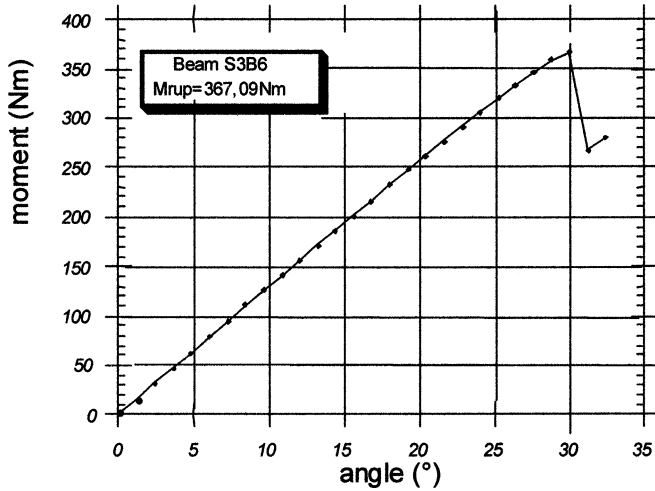


Fig. 4. *M-θ* curves for monotonous test

Table 2. Cyclic tests: variation in amplitude

Beam	Amplitude		Frequency (Hz)	Remarks
	%	Nm		
S1.13	30	110.64	0.250	
S2.18	30	135.52	0.204	
S2.30	30	135.52	0.204	
S2.20	30	135.52	0.204	
S3A.28	30	117.45	0.236	
S3B.36	30	117.45	0.236	
S1.18	35	129.08	0.214	
S1.11	40	147.52	0.187	
S3B.12	40	156.60	0.177	
S3A.15	40	156.60	0.177	
S1.7	45	165.96	0.166	
S1.10	50	184.41	0.150	
S3A.39	50	195.75	0.141	
S3B.13	50	195.75	0.141	Fractured at cycle 1500
S1.9	55	202.85	0.136	Cracked
S1.15	50	184.41	0.150	Cracked
S1.3	47	173.34	0.160	
S1.14	50	184.41	0.150	Cracked
S1.6	48	177.02	0.156	
S1.8	49	180.72	0.153	
S1.5	50	184.41	0.150	
S1.1	55	202.85	0.136	
S1.2	60	221.29	0.125	
S3B.29	60	234.89	0.118	Fractured at cycle 900
S3A.4	60	234.89	0.118	Fractured at cycle 500
S3A.11	70	274.04	0.101	Fractured at cycle 10
S3B.16	70	274.04	0.101	Fractured at cycle 8
S3A.18	80	313.19	0.088	Fractured at cycle 21
S3B.22	80	313.19	0.088	Fractured at cycle 3
S3A.21	90	352.34	0.079	Fractured at cycle 2
S3B.35	90	352.34	0.079	Fractured at cycle 4

Cyclic tests

The cyclic tests were performed with control of moment, and a triangular signal was used. Periodic measurements of the temperature and humidity of small samples of the wood stacked with the beams permitted us to note even small variations in these two physical parameters. Finally, because of the large number of specimens and to limit the total time of testing, we set a conventional limit of 2000 cycles for each test.

The results are shown in Table 2. Figures 5 and 6 show two types of limit behavior of the beams: (1) adaptation for low amplitudes; and (2) ratchet for the higher amplitudes up to 50% of the middle monotonous moment of failure.

The evolution of the beam response (i.e., the torsion angle), according to the number of cycles for different values of the moment amplitude, show good stabilization for values lower than 50% of the middle failure moment; beyond of this value, material damage is obvious before the fixed limit (2000 cycles), shown by a progressive increase in the torsion angle that causes beam failure after a cycle number that decreases with the amplitude.

Testing low-amplitude, polynomial equations of the shape $y = a + b \cdot x^c$ proved to be better for smoothing the experimental points (Fig. 7). As soon as a crack appears in the beam, the aspect of the angle–cycles curve becomes exponential, and failure occurs after a reduced number of cycles.

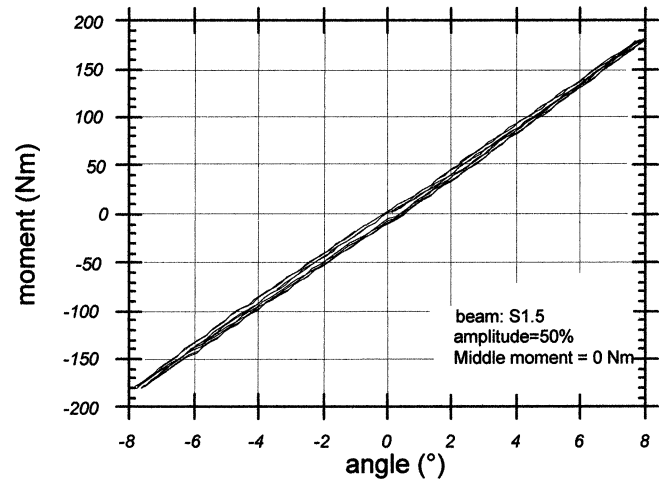


Fig. 5. Evolution of the hysteresis loop (accommodation) (cycles 1 to 2000)

Figure 8 represents the variation in the number of cycles until failure with the loading amplitude. These tests showed the existence of a limit of the amplitude adjoining the 50% at which failure occurs. Over this limit, the number of cycles until failure decreases exponentially with the increase in amplitude.

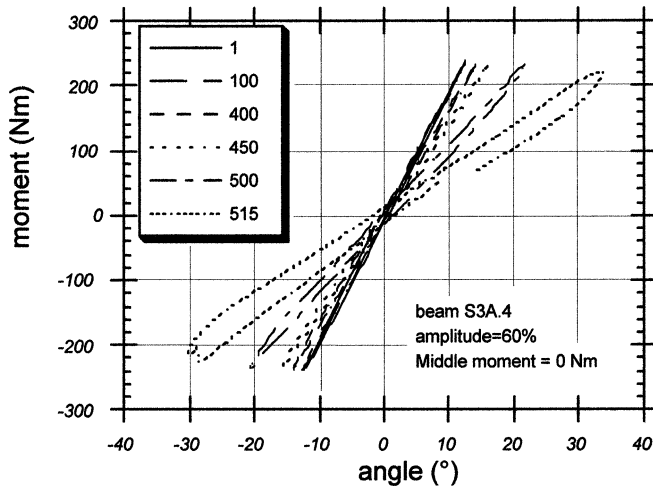


Fig. 6. Evolution of the hysteresis loop (Ratchet) (cycles 1 to 515)

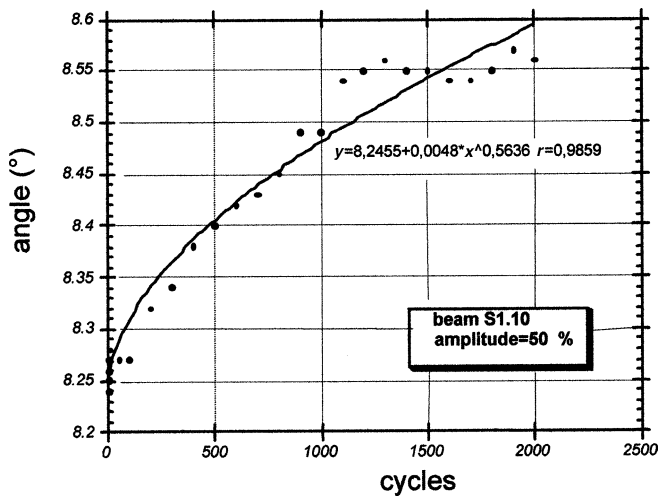


Fig. 7. Variation of the maximum angle according to the number of cycles

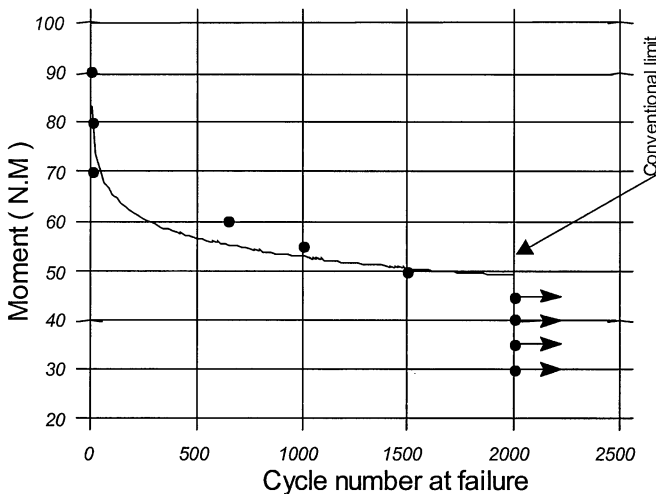


Fig. 8. Variation of the number of cycles until failure according to the amplitude

Conclusions

The behavior of glued-laminated wood beams in torsion for various loading programs and the influence of the various loading parameters on this behavior are clarified. Beams show that, under monotonous torsion, their behavior is almost fragile. Failure occurs consequent to propagation of a longitudinal crack that starts in the wood on the large face of the beam, as predicted by the theory. Under cyclic loading, amplitude appears to be one of the most influential factors affecting the response of the beams. At nil middle moment, beams have a steady behavior for low amplitude, and they accommodate. The lost energy during each cycle increasingly damages the beam, and failure intervenes only after a large number of cycles. The evolution of the distortion according to the number of cycles is of the shape $y = a + b \cdot x^c$. Failure occurs only for amplitudes adjoining 50% of the middle failure moment, and it is the same type of that observed with the monotonous tests.

We conclude that, based on this experimental investigation, much remains to be done theoretically and experimentally to understand the behavior of wood in torsion. Results of other tests will help illuminate the problem.

References

1. Kollman FP, Cote WA (1968) Principles of wood science and technology. Springer Verlag, Berlin Heidelberg New York
2. Bodig J, Jayne BA (1982) Mechanics of wood and wood composites. Van Nostrand Reinhold, New York
3. Guitard D (1987) Mécanique du matériau bois et composites. Editions Cepadues, Toulouse
4. Guitard D, Seichepine JL (1980) Analyse du comportement élastique du matériau bois, mise au point d'une méthode de détermination de la matrice de rigidité du Hêtre. Final report of a D.G.R.S.T contract
5. Gunnerson RA, Goodman JR, Bodig J (1973) Plate tests for determination of elastic parameters of wood. Wood Sci 5:241–248
6. Wu, Chung, Biblis EJ (1977) New approach for determination of elastic constants of orthotropic wood base plates by strip bending and plate twisting. Wood Sci 9:329–334
7. Seichepine JL (1980) Mise au point d'une méthode expérimentale destinée à l'identification de la matrice des complaisances élastiques de solides anisotropes: application au matériau bois. PhD thesis, National Polytechnic Institute of Loraine
8. Bucur V (1981) Détermination du module d'Young du bois par une méthode dynamique sur carotte de sondage. Ann Sci For Versailles 38(2)
9. Murdry M, Launay J, Preziosa C, Gilletta F (1985) La mesure des constantes élastiques des matériaux par goniométrie ultrasonore. Presented at the 17th French yearly symposium of rheology, E.N.P.C, Paris, 1985
10. Schniewind AP, Barrett JD (1972) Wood as a linear orthotropic viscoelastic material. Wood Sci Technol 6:43–57
11. Kellog RM (1958) Strain behavior of wood subject to repetitive stressing in tension parallel to the grain. For Prod J 8:301–307
12. Cariou JL (1987) Caractérisation d'un matériau viscoélastique anisotrope: le bois. PhD thesis, University of Bordeaux
13. Foudjet A (1986) Contribution à l'étude rhéologique du matériau bois. PhD thesis, University Claude Bernard Lyons
14. King EG (1961) Time-dependent strain behavior of wood in tension parallel to the grain. For Prod J 11:156–165
15. King EG (1958) The strain behavior of wood in tension parallel to the grain. For Prod J 8:330–334

16. King EG (1957) Creep and other strain behavior of wood in tension parallel to the grain. For Prod J 7:324-330
17. Kellog RM (1960) Effect of repeated loading on tensile properties of wood. For Prod J 10:586-594
18. Timoshenko S, Goodier JN (1961) Theorie de l'élasticité. Librairie Polytechnique Ch. Beranger, Paris and Liege
19. Sokolnikoff IS (1983) Mathematical theory of elasticity. Krieger Publishing, Melbowne, FL